

Simulation study on the thermal insulation performance of liquid hydrogen transport pipelines

Yihan Tian^{1,2}, Zhijian Zhang^{1,2}, Zhaozhao Gao^{1,4}, Biao Yang¹, Chen Cui^{1,2}, Jia Guo^{1,2}, Liubiao Chen^{1,2,4,*}, Junjie Wang^{1,2,3}

¹ State Key Laboratory of Cryogenic Science and Technology, Technical Institute of Physics and Chemistry, Chinese Academy of Sciences, Beijing 100190, China;

² University of Chinese Academy of Sciences, Beijing 100049, China;

³ Zhonglv Zhongke Energy Storage Technology Co., Ltd., 18 Lishi Hutong, Dongcheng District, Beijing 100020, China;

⁴ Institute of Optical Physics and Engineering Technology, Qilu Zhongke, Licheng District, Jinan 250100, China;

* Corresponding author. E-mail: chenliubiao@mail.ipc.ac.cn (Dr. Liubiao Chen)

ABSTRACT. Hydrogen engines, compared to traditional gas engines, offer higher energy density and combustion efficiency. These advantages not only significantly enhance the propulsion performance of aircraft but also extend their range, presenting substantial potential for applications in the aviation sector. As a crucial component of hydrogen engine systems, the design and performance of liquid hydrogen transport pipelines directly influence the efficiency and safety of hydrogen delivery, making them essential for ensuring a stable supply and efficient utilization. This study focuses on the thermal insulation performance of liquid hydrogen transport pipelines by developing a multi-physics coupling model that incorporates heat conduction, radiation, and convection. Through simulation studies based on vacuum insulation technology, the contributions of different structural components to the total heat loss are quantitatively evaluated, and the effects of vacuum level, support structure, and thermal bridge design on the overall heat loss of the pipeline are further investigated. The findings provide theoretical guidance for optimizing the insulation system of liquid hydrogen transport pipelines, which is crucial for improving hydrogen storage and transportation efficiency, reducing cold energy loss, and advancing the industrial application of hydrogen energy technologies.

1. Introduction

With the increasing demand for cleaner and more efficient propulsion technologies in aviation, hydrogen engines have emerged as a promising alternative to conventional gas turbines. They offer enhanced propulsion performance and extended flight range, making them highly attractive for next-generation aerospace systems. Among various hydrogen storage and delivery methods,



liquid hydrogen stands out for its high energy density [1]. However, the cryogenic conditions required for LH₂ storage and transport pose significant engineering challenges, especially in maintaining thermal insulation in transfer pipelines, which is essential for stable and efficient fuel delivery. The ITER cryogenic system, one of the world's largest, has spurred extensive research into cryogenic pipeline design [2]. M.V. Krishnamuthy et al. [3] confirmed that higher vacuum levels reduce liquid nitrogen evaporation, while A. Dubner et al. [4] used finite element analysis to optimize thermal performance and support layout.

This research focuses on the thermal insulation performance of liquid hydrogen transfer pipelines. A multi-physics simulation model is developed to evaluate the overall heat transfer characteristics of the pipeline. Moreover, the thermal contribution of each structural component to the heat leakage is quantitatively analyzed. The findings provide theoretical guidance for optimizing the insulation system of liquid hydrogen pipelines, facilitating the reduction of cryogenic energy losses and improving hydrogen delivery efficiency.

2. Model and boundary conditions

As shown in Fig. 1, the liquid hydrogen transport pipe has a total length of 830 mm and consists of an inner and an outer pipe, with inner diameters of 18 mm and 38 mm, respectively, and wall thicknesses of 1 mm. A vacuum layer between them serves as the primary thermal insulation, effectively suppressing convective and conductive heat transfer. To maintain the inner pipe's stability and alignment, low-conductivity PTFE supports (10 mm thick) are used. Thermal bridges connect the inner and outer pipes at both ends, ensuring mechanical linkage while minimizing axial heat conduction by optimizing heat transfer paths. The sealing joints adopt a spherical metal structure, 80 mm in length. To relieve stress from thermal expansion and contraction under cryogenic conditions, a corrugated pipe section is added to the inner pipe's middle, providing axial flexibility and improving the system's structural reliability and service life.

The main thermal loads of the pipe include radiative heat transfer and residual gas conduction heat transfer between the inner and outer pipes, solid conduction through thermal bridges, support structures, and sealing joints, as well as convective heat transfer between the inner pipe and liquid hydrogen, and between the outer pipe and the ambient environment. To facilitate numerical simulation, several simplifications are made, and the boundary conditions are set as follows:

(1) The inner wall temperature of the inner pipe is set to the liquid hydrogen temperature, i.e., 20 K; (2) The convective heat transfer coefficient between the outer pipe and the external environment is set to 5 W/(m²·K) [5]; (3) The sealing joint is wrapped with a 20 mm thick insulation sponge with a thermal conductivity of 0.03 W/(m·K).

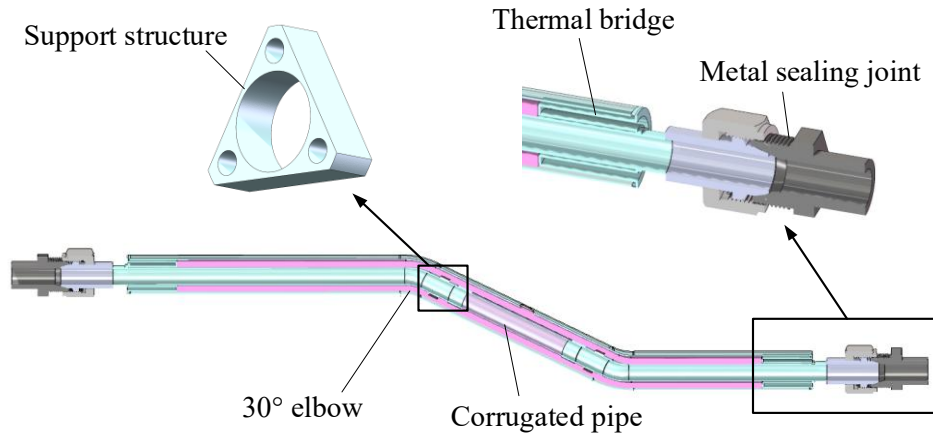


Figure 1. Structure schematic of liquid hydrogen transport pipe.

3. Heat transfer mechanisms

The heat transfer between the inner and outer tubes includes not only solid conduction, but also radiative heat transfer and residual gas conduction. The radiative heat transfer can be calculated using the Stefan–Boltzmann equation:

$$q_{rad} = \varepsilon \sigma (T_{out}^4 - T_{in}^4) \varphi$$

where q_{rad} is the radiative heat transfer rate; σ is the Stefan–Boltzmann constant; φ is the relative radiation angle factor, which can be taken as $\varphi = 1$; $\varepsilon = \left[\frac{1}{\varepsilon_{in}} + \frac{1 - \varepsilon_{in}}{\varepsilon_{out}} \left(\frac{d_{in}}{d_{out}} \right) \right]^{-1}$ is the overall emissivity, where ε_{in} and d_{in} are the emissivity and diameter of the outer surface of the inner pipe, respectively, and ε_{out} and d_{out} are the emissivity and diameter of the inner surface of the outer pipe, respectively.

The residual gas conduction can be calculated using the following equation:

$$q_{gc} = k \alpha P_{vac} (T_{out} - T_{in})$$

where q_{gc} is the residual gas conduction heat transfer rate; P_{vac} is the pressure in the vacuum jacket; $\alpha = \left[\frac{1}{\alpha_{in}} + \frac{d_{out}}{d_{in}} \left(\frac{1}{\alpha_{in}} - 1 \right) \right]^{-1}$ is the thermal accommodation coefficient; $k = \frac{\tau + 1}{\tau - 1} \sqrt{\frac{R}{8\pi M T}}$ is the thermal conductivity of gas molecules, where τ is the specific heat ratio, R is the ideal gas constant, and M is the molecular mass.

4. Results and discussion

4.1 Proportion of heat leakage

The simulation results show that the total heat leakage of this pipeline model is approximately 6.23W (7.51W/m). Fig. 2 illustrates the proportion of heat leakage from each component relative to the total system heat loss when the vacuum level is 10^{-3} Pa. The thermal bridge, serving as a

critical structural element directly connecting the inner and outer pipes, experiences a significant temperature gradient at both ends and exhibits the highest heat leakage, representing 32% of the total. Due to their structural characteristics and the thermal conductivity of their materials, sealing joints and support structures also contribute to the overall heat loss. Radiative heat transfer between the inner and outer pipes accounts for 16.765% of the total heat loss. In addition, the contribution of residual gas conduction is minimal and can be essentially neglected.

In summary, radiative heat transfer between the inner and outer pipes, residual gas conduction in the vacuum jacket, and solid conduction through connecting components together constitute the main heat leakage pathways of the system. Among these, solid conduction through the connecting components is particularly significant, accounting for approximately 78.4% of the total heat loss. Therefore, subsequent design optimizations should focus on improving insulation and thermal isolation for these key pathways to effectively reduce overall heat losses.

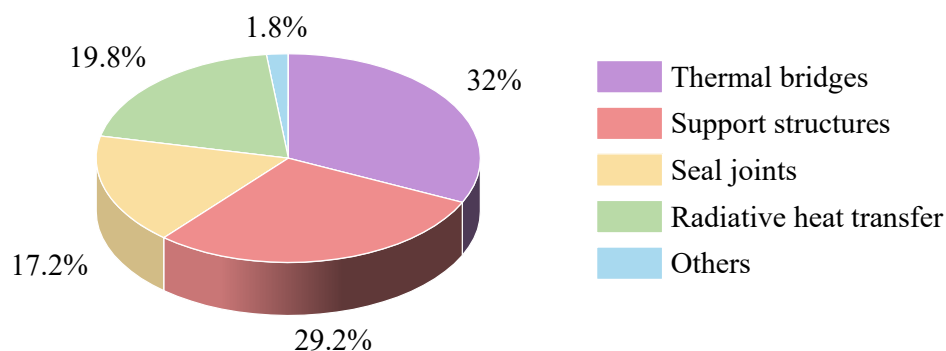


Figure 2. Contributions of different components.

4.2 Effect of different vacuums

Fig. 3 illustrates the variation of residual gas conduction heat leakage in the vacuum jacket as a function of vacuum pressure. Under high-vacuum conditions, gas molecules are in the free-molecular regime, where the mean free path is much greater than the characteristic dimension. In this regime, residual gas conduction is negligible and the heat leakage remains relatively constant. As the vacuum level deteriorates, gas molecules progressively enter the temperature-jump or transitional regime, where intermolecular collisions become more frequent and the heat load increases approximately linearly with pressure. When the gas transitions into the continuum regime, heat transfer is primarily governed by the potential energy of the molecules and the energy exchange during collisions. Once the continuum regime is fully established, the gas conduction heat leakage approaches a steady value. Specifically, when the pressure rises from 10^{-3} Pa to 10^4 Pa, the gas conduction heat leakage increases by roughly five orders of magnitude. These results highlight that vacuum degradation has a pronounced effect on heat leakage,

underscoring the importance of maintaining a high vacuum level (below 10^{-3} Pa) in practical applications.

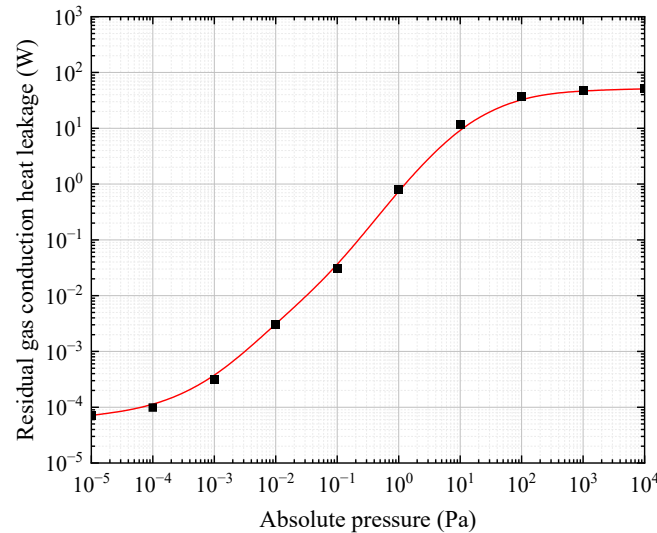


Figure 3. Residual gas conduction heat leakage under different vacuum.

4.3 Design of support structures

The thermal insulation performance of support structures depends not only on material selection but also, crucially, on geometric design. As shown in Fig. 4, simulations are conducted for three common cryogenic pipeline supports, triangular, square, and annular, with heat leakage values of 0.921 W, 0.904 W, and 0.929 W, respectively. The square support demonstrated the best insulation performance, benefiting from evenly distributed contact points and longer heat conduction paths, which effectively reduce thermal transfer. This makes it well-suited for high-performance cryogenic systems requiring superior insulation. The triangular support, while slightly less efficient thermally, features a simpler structure and fewer contact points, offering advantages in manufacturing and assembly. It is ideal for applications prioritizing cost-effectiveness and simplicity. The annular support exhibited the highest heat leakage due to its larger conductive surface area, despite providing strong mechanical stability. It is better suited for scenarios where structural robustness is more critical than thermal performance.

In conclusion, square supports are optimal for minimizing thermal loss, triangular supports offer a balance of thermal performance and structural simplicity, and annular supports are preferable when mechanical strength is paramount.

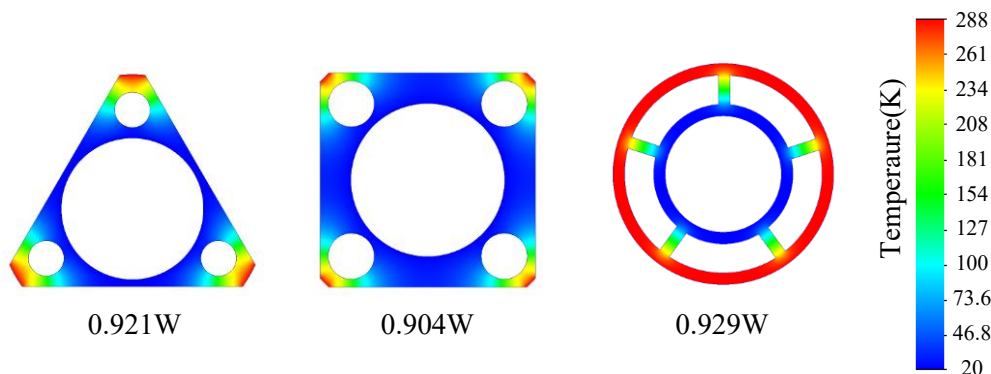


Figure 4. Temperature distribution and heat leakage of different support structures.

4.4 Structure of thermal bridge

As a critical component connecting the inner and outer tubes, the thermal bridge experiences a substantial temperature gradient and thus serves as a significant contributor to overall heat leakage. As shown in Fig. 5, the variation of heat leakage through the thermal bridge with respect to its length and thickness reveals clear trends. Specifically, increasing the length of the thermal bridge extends the heat conduction path, thereby reducing heat leakage. Conversely, increasing the thickness of the thermal bridge leads to a substantial rise in heat leakage, indicating that a greater cross-sectional area enhances thermal conduction and thus intensifies heat loss.

Therefore, to effectively minimize the heat leakage of the thermal bridge, one feasible strategy is to increase its length while reducing its thickness. Additionally, the figure illustrates the interactive effects between length and thickness. For thicker thermal bridges, length has a more pronounced impact on heat leakage; whereas for shorter bridges, thickness plays a more dominant role. It is also noteworthy that the relationship is not strictly linear due to the influence of adjacent structural components.

These observations suggest that the design of the thermal bridge must consider both geometric parameters, namely length and thickness, in a coordinated manner. It is essential to balance the mechanical strength requirements with the thermal insulation performance. This comprehensive optimization strategy is particularly important in cryogenic transfer systems, where minimizing thermal loads and improving both energy efficiency and system stability are critical objectives.

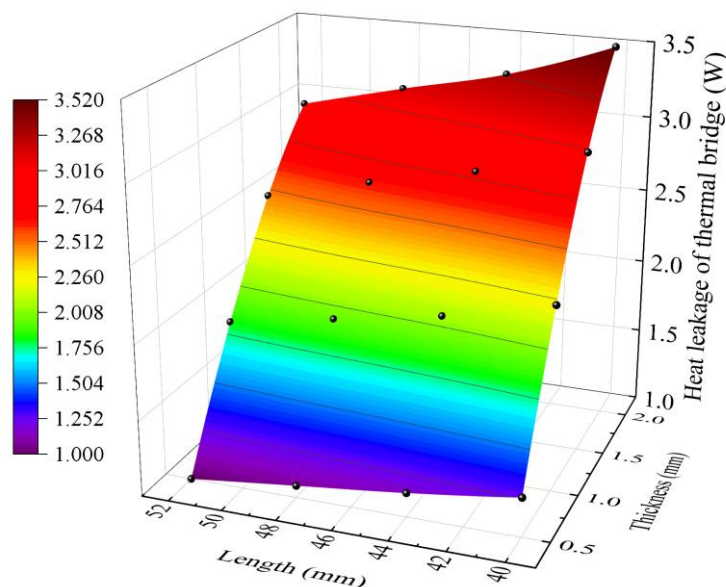


Figure 5. Heat leakage of different design of thermal bridge.

5. Conclusions

In this study, a multi-physics simulation model coupling heat conduction, convection, and radiation was developed to systematically analyse the thermal insulation performance of liquid hydrogen transfer pipelines. The results indicate that the heat leakage of this pipeline model is approximately 7.51 W/m. Among the various heat loss paths, solid conduction contributes the most, accounting for 78.4% of the total heat loss, followed by radiative heat transfer between the inner and outer pipes. Degradation of vacuum significantly increases heat loss, primarily due to the pronounced rise in residual gas conduction at higher vacuum pressures. In terms of structural optimization, a single square support exhibits a heat leakage of 0.904 W, showing superior insulation performance compared to triangular and ring-shaped supports. Furthermore, the length and thickness of the thermal bridge exhibit an interactive effect on heat leakage, with thinner and longer thermal bridges effectively reducing axial conduction.

References

- [1] Moradi R and Groth K M 2019 *Inter. J. Hydrogen Energ.* **44** 12254-69
- [2] Serio L, Chalifour M, Kalinin V, et al 2008 *ICEC 22-ICMC.* 607-612.
- [3] Krishnamurthy M V, Chandra R, Jacob S, et al 1996 *Cryogenics.* **36** 435-441.
- [4] Dubner A, Zacharias D, Nagel M, et al 2009 *Fusion Eng. Des.* **84** 694-697.
- [5] Kawano K, Hamada K, Kato T, et al 1997 *ICEC16-ICMC.* 493-496.